Title	High temperature ferromagnetic ordering in c-axis oriented ZnO:Mn nanoparticle thin films by tailoring substrate temperature
Author(s)	Usman Ilyas, P. Lee, T. L. Tan, R. V. Ramanujan, Sam Zhang, R. Chen, H. D. Sun and R. S. Rawat
Source	*International Journal of Modern Physics: Conference Series, 32*(2014), 1460341
Published by	World Scientific

doi: 10.1142/S201019451460341X

Plasma Science and Applications (ICPSA 2013)
International Journal of Modern Physics: Conference Series
Vol. 32 (2014) 1460341 (11 pages)

DOI: 10.1142/S201019451460341X

World Scientific
www.worldscientific.com

High temperature ferromagnetic ordering in c-axis oriented ZnO:Mn nanoparticle thin films by tailoring substrate temperature

Usman Ilyas*

National Institute of Education, Nanyang Technological University, 1 Nanyang Walk, 637616 Singapore
Department of Physics, University of Engineering & Technology Lahore 54890, Pakistan
**iusman82@gmail.com*

P. Lee and T. L. Tan

National Institute of Education, Nanyang Technological University, 1 Nanyang Walk, 637616 Singapore

R. V. Ramanujan

School of Material Science and Engineering, Nanyang Technological University, 639798 Singapore

Sam Zhang

School of Mechanical and Aerospace Engineering, Nanyang Technological University, 639798 Singapore

R. Chen and H. D. Sun

Division of Physics and Applied Physics, School of Physical and Mathematical Sciences, Nanyang Technological University, 21 Nanyang Link 637371, Singapore

R. S. Rawat

National Institute of Education, Nanyang Technological University, 1 Nanyang Walk, 637616 Singapore

Published 13 August 2014

This study reports the enhanced ferromagnetic ordering in ZnO:Mn nanoparticle thin films, grown at different substrate temperatures using pulsed laser deposition. The optimum growth conditions were deduced from X-ray, photoemission and magnetic measurements. The X-ray measurements reveal that there was an optimum substrate temperature where the thin films showed relatively stronger texture, better crystallinity and lower strain. Substrate temperature tuned the deep level recombination centers in ZnO:Mn, which changed the optical quality by altering the electronic structure. The M-H curves, in the present study, revealed superior ferromagnetic response of 20-nm sized particles in ZnO:Mn thin film grown at a substrate temperature of 450 °C. Ferromagnetic ordering becomes weaker at higher/lower substrate temperatures due to the activation of native defects in ZnO host matrix.

Keywords: Spintronics; ZnO:Mn nanoparticle thin films; structural defects; substrate temperature.

1. Introduction

The subject of dilute magnetic semiconductors (DMS), for a reliable spin polarized material, has attracted great research interest for being a ferromagnetic semiconductor with promising experimental properties to be used in spintronics. The emerging field of spintronics has generated a wide spread interest because of its potential to provide new functionalities and enhanced performance in conventional electronic devices.[1] Oxide materials, with their wide band gaps, provide a convenient platform to study the spin based functionality, and are predicted to exhibit room temperature ferromagnetism (RTFM) with higher Curie temperatures.[2] ZnO based DMS have been studied extensively after the theoretical work of Dietl, predicting the RTFM in wide band gap semiconductors.[2]

Numerous experimental investigations have shown controversial results about the origin of ferromagnetism in ZnO:Mn based DMS. The transition metals (TM) inside the ZnO lattice, structural defects, secondary phases or an interfacial double-exchange mechanism at the diffusion front of Zn cations; have been reported to cause the ferromagnetism in ZnO:TM materials.[3-5] The ferromagnetic ordering in ZnO:Mn thin films is reported to be due to p-type conductivity, with holes carrier concentration of the order of ~ 10^{+16}-10^{+17} cm^{-3},[6-8] as well as due to structural defects.[9, 10] Deep acceptor levels, low dopant solubility and high self-compensation in ZnO thin films are thought to be a bottleneck limiting RTFM to lower temperatures.[11] Moreover, structural defects like oxygen vacancies (V_o) exhibited by deep level emission (DLE) spectra also contribute towards ferromagnetic exchange coupling of Mn in ZnO host matrix, ultimately leading to defect mediated RTFM.[5] Therefore, the quenching of oxygen vacancies in non-stoichiometric ZnO:Mn thin films, is of great importance to improve the ZnO stoichiometry and reduce their contribution towards ferromagnetism. The control of carrier concentration (structural defects) to make RTFM to be originated by the indirect ferromagnetic exchange coupling is a pre-requisite for spintronics applications. The present study reports enhanced ferromagnetic response in ZnO:Mn thin films grown by pulsed laser deposition under argon-oxygen admixture ambient gas due to substrate temperature-dependent tuning of stoichiometry.

2. Experimentation

ZnO:Mn thin films, with oxygen rich stoichiometry, were grown by pulsed laser deposition (PLD) technique using 2nd harmonic Nd:YAG laser (532 nm, 38 mJ). The ZnO:Mn targets for PLD were pelletized and sintered from nano-crystalline ZnO:Mn powder synthesized through a wet chemical method, using growth and processing conditions reported elsewhere.[12, 13] The PLD vacuum chamber was evacuated to a base pressure of 10^{-6} mbar. The thin film samples were deposited using argon-oxygen admixture (with $Ar:O_2$=9:1) at 2.5 mbar on Si (100) substrate for a constant ablation period of 30 min along with in-situ substrate heating. The substrate temperatures of 400, 450 and 500 °C were used and the corresponding depositions are herein after referred as ISA-400, ISA-450 and ISA-500, respectively.

3. Results and Discussions

3.1 *Structural analysis*

Figure 1 shows the X-ray diffraction (XRD) spectra of nanocrystalline ZnO:Mn thin films, obtained using a SIEMENS D5005 Cu Kα (1.5406 Å) X- ray Diffractometer, with the preferential growth along c-axis (002). A marked increase in (002) diffraction peak intensity was observed for ISA-450 in comparison to other samples which in turn indicates the improved crystalline quality of this sample. The average crystallite sizes, estimated from peak broadening using the Scherer's formula, are found to be 12.0 $\pm$ 1.3 nm, 17.8 $\pm$ 1.1 nm and 12.9$\pm$ 1.0 nm for ISA-400, ISA-450 and ISA-500 samples, respectively, exhibiting the nanocrystalline nature of the thin films. The increased crystallite size for ISA-450 is due to the reduction in the concentration of point defects and rearrangement of crystal grains.[14]

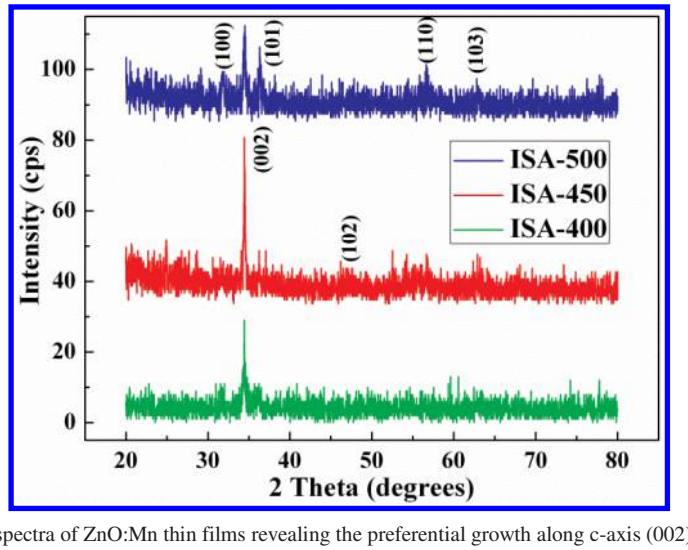

Fig. 1. XRD spectra of ZnO:Mn thin films revealing the preferential growth along c-axis (002) orientation.

Small signatures of (100) and (101) planes were also observed along with the c-axis oriented (002) peak in ISA-500 revealing its polycrystalline nature. This might be due to the resistance offered by Mn atoms for the growth of ZnO along c-axis at this temperature.[15] Moreover, minimum diffraction peak intensity for ISA-500 with reduced crystallite size points to enhanced concentration of point defects (diffusion of oxygen at the interstitial sites), which reduces crystalline quality. The re-sputtering of neutral oxygen atoms and surface oxidation of the target (due to excess oxygen) are also reported to hinder grain growth causing the reduction in c-axis (002) orientation.[15] The relative change in lattice constant 'c' was used to estimate the strain in the thin films grown at different substrate temperatures. The strain [$\varepsilon = c_{film}\text{-}c_{bulk}/\ c_{bulk}$],[15] which is directly related to the structural defects, was estimated to be 0.86×10^{-3}, 0.18×10^{-3} and 1.2×10^{-3} for ISA-

400, ISA-450 and ISA-500, respectively, suggesting residual compressive stress. The compressive stress is due to the incorporation of Mn at the lattice sites of Zn and activation of structural defects in ZnO host matrix. Moreover, the ambient gas particles (argon and oxygen ions), having sufficient energies, cause implantation or displacement of surface atoms which can lead to significant stress levels.[15] The thin film grown at substrate temperature of 450 °C seems to have smallest strain, due to the improved homogeneity and stoichiometry of the thin film. The above results indicate that there is an optimum substrate temperature (450 °C) where the film shows stronger texture and better nano-crystallinity. Lower or higher temperatures would lead to increased stress levels due to the concentration and activation of structural defects resulting in deterioration in optical and crystalline quality of the thin films.

3.2 *Compositional analysis*

Elemental oxidation states and surface stoichiometry (chemical bond configuration) of the thin film samples were identified, using X-ray photoelectron spectroscopy (XPS) equipped with a focused monochromatic Al-Kα (1486.6 eV) X-ray beam, by analyzing Zn 2p, O 1s and Mn 2p core level spectra. The stoichiometry of all thin films was found to be oxygen rich with Zn/O<1, that is different from most of the literature in which the stoichiometry is reported to be zinc rich[16]. Figure 2 shows the deconvoluted (using Gaussian fitting) core level XPS spectra of the thin film grown at substrate temperature of 450 °C (ISA-450). The main core level XPS spectrum of Zn $2p_{3/2}$ centered at ~ 1020.4 eV, showing slightly asymmetrical features [refer Fig. 2], indicates the existence of Zn in its multiple-oxidation states.

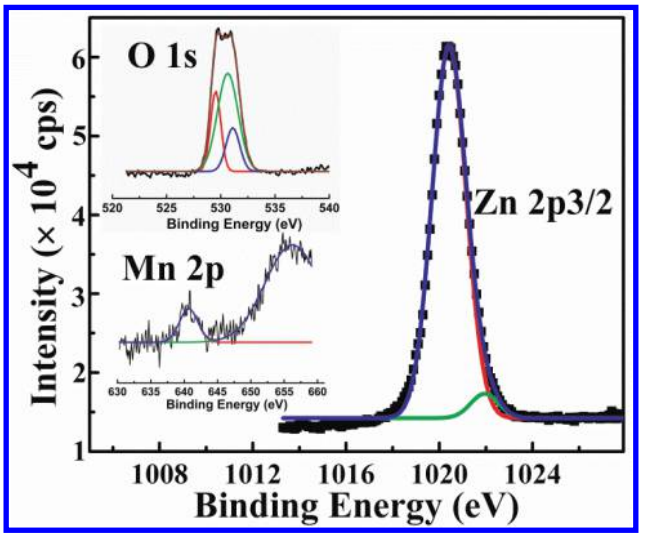

Fig. 2. Core level XPS spectra of Zn $2p_{3/2}$, O 1s and Mn 2p of ISA-450.

The deconvoluted Zn $2p_{3/2}$ core level XPS spectrum shows two peaks, centered at ~ 1020.4 eV and ~ 1021.9 eV, corresponding to different oxidation states of Zn. The lower energy peak in the deconvoluted spectrum is attributed to the Zn^{2+} ion array surrounded by O^{2-} ions in the hexagonal ZnO and is termed as the oxide form of Zn.[17, 18] The deconvoluted peak centered at the higher binding energy side is related to metallic zinc. Thin films with more oxygen vacancies (V_o) reduce stoichiometry and almost approach to metallic nature [19]. By estimating the relative area under the deconvoluted peaks, it was found that the relative contribution from the peak centered towards the lower energy side (~1020.4 eV) was maximum (~ 95%) in ISA-450, which indicates enhanced Zn-O bonding. The relative concentration of oxide form of zinc in ISA-400 and ISA-500 was estimated to be ~ 90 % and 57%, respectively. The maximum Zn-O bonding in ISA-450, exhibiting better homogeneity, favors the strong indirect sp-d ferromagnetic double-exchange coupling in carrier mediated ZnO:Mn thin films, resulting in enhanced ferromagnetic signal [17] for this sample.

The inset in Fig. 2 shows the deconvoluted O 1s core level XPS spectrum comprising of three binding energy peaks centered at ~529.5, 530.6 and 531.1 eV. The peak centered at ~ 531.1 eV is related to the presence of oxygen in oxygen deficient regions in ZnO host matrix[12]. Therefore, the variation in the relative area under the curve of this peak is related to the variation in the concentration of oxygen vacancies (V_o). The relative concentration of V_o was estimated to be lower (~ 18%) in ISA-450 than other samples in which the relative concentration was estimated to be ~ 60%. The peak centered at 530.6 eV can be attributed to the O^{2-} ions in Zn-O bond (58%) which further justifies better stoichiometry in ISA-450 as compared to other samples under investigation.

The core level XPS spectrum of Mn 2p, exhibiting $2p_{3/2}$ and $2p_{1/2}$ spin-orbit doublet at 640.8 eV and 656.2 eV, is shown in Fig. 2 (inset). These results indicate that the doped Mn is in its divalent state (Mn^{2+}), which rules out the possibility of nanoclustering or any impurity phase formation of Mn. It has been reported that the Mn nearest neighbor short range exchange interaction (ferromagnetic/anti-ferromagnetic) is strongly dependent on the concentration of structural defects. [20, 21] Therefore, the optimum concentration of structural defects with better homogeneity of Mn and improved stoichiometry (Zn-O) is favorable to enhance the ferromagnetic ordering in this sample.

3.3 *Morphological analysis*

Surface features and variation in nanoparticle size were studied using JEOL JSM 6700 field emission scanning electron microscope (FESEM). Figure 3 shows the FESEM micrographs of thin film samples revealing the formation of nano-sized particles on ISA-400 and ISA-450 while the sample ISA-500 exhibits the nanoplate-like morphology. The average particle size was found, using image processing (image J®) software, to increase from ~ 12.7 ± 0.3 nm for ISA-400 to ~ 21.6 ± 0.6 nm for ISA-450, in turn, revealing their narrow size distribution. In addition the size of nanoplate like structures in ISA-500 was estimated to be ~ 37.64 ± 2.7 nm. The increase in particle size and formation of nanoplate

like structures with increasing in-situ annealing temperature can possibly be attributed to the fact that with increasing in-situ annealing temperature, the process of coalescence takes place in which smaller particles mix together to form larger particles (in case of ISA-450) and nanoplate like structures (in case of ISA-500).

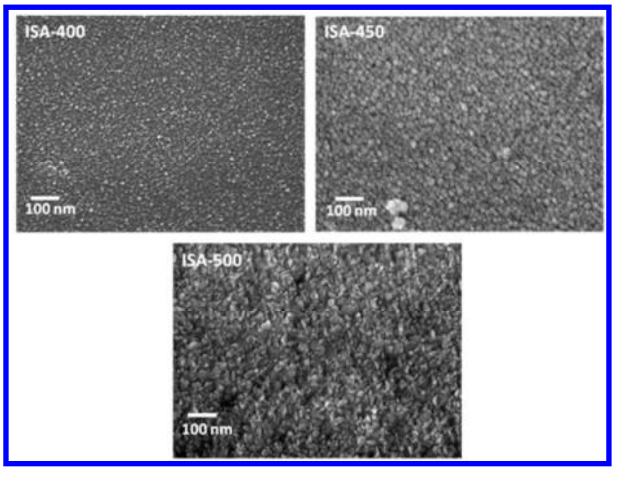

Fig. 3. FESEM micrographs of ZnO:Mn thin films exhibiting ZnO:Mn nanoparticles and nanoplates.

3.4 *Optical analysis*

Figure 4 shows the room temperature photoluminescence (RT PL) spectra, measured using He-Cd (325 nm, 10 mW) laser, of the nanocrystalline ZnO:Mn thin films grown at different substrate temperatures. RT PL spectra revealed two emission bands in UV and

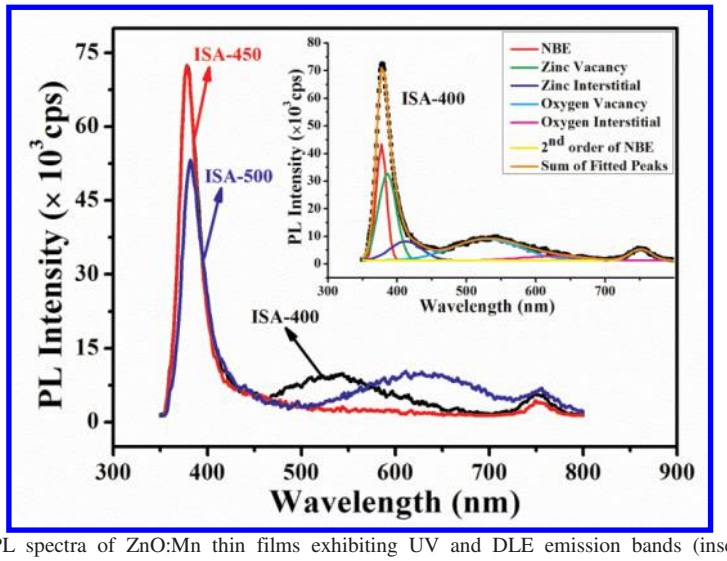

Fig. 4. RT PL spectra of ZnO:Mn thin films exhibiting UV and DLE emission bands (inset shows the deconvoluted PL spectra of ISA-400 exhibiting the presence of structural defects).

visible spectral regions. The near band edge (NBE) emission centered at ~ 380 nm has been observed in all PL spectra which originates from band to band transitions in optical band gap of ZnO.[21] The broad deep level emission (DLE) in visible spectral regions are closely related to structural defects, like oxygen vacancies, oxygen interstitials, zinc vacancies and zinc interstitials[13, 22] in ZnO.

The deconvulution of broad DLE spectra (using Gaussian function) was used to estimate the relative concentration of structural defects in ZnO. The DLE spectrum for ISA-400 was deconvoluted into five peaks (shown in inset of Fig. 4) centered at 379, 390, 412.4, 528.4 and 623.5 nm which are attributed to near band edge emission between the optical band gap of ZnO (46.7 %), singly ionized zinc vacancy (35.1%), zinc interstitials (7.6 %) oxygen vacancy (8.6%) and oxygen interstitials (1.7%), respectively.[23] For the sample grown at a substrate temperature of 500 °C, the presence of oxygen vacancies and oxygen interstitials were observed with their relative concentrations of 33.8% and 66.1%, respectively. The presence of oxygen interstitials can also alter exchange coupling of Mn in ZnO host matrix.[24] The stronger NBE emission for ISA-450 with minimum DLE spectra points to enhanced stoichiometric ZnO formation, which, in turn, is responsible for the improved optical quality of the thin film. Moreover, improved NBE emission in thin film grown at substrate temperature of 450 °C (ISA-450) is attributed to its higher crystallinity resulting from the reduction in compressive strain and point defects which is consistent with XRD results.

These results can be understood by assuming that the in-situ substrate temperature controls the number of deep level recombination centers or it activates new states that provide alternative decay paths, hence affecting the PL emission. In both cases, it is inferred that growth temperature alters the electronic structure of the thin films, modifying their energy levels. Therefore, 450 °C is found to be an optimum substrate temperature, in our case, for the growth of good quality nanocrystalline ZnO:Mn thin film favorable for enhanced RTFM. On the contrary, lower or higher growth temperatures will lead to the activation of structural defects, like vacancies and interstitials of oxygen, which will deteriorate the crystalline, optical and magnetic quality of thin film samples.

3.5 Magnetic properties

Figure 5 illustrates the dependence of magnetization, measured using a Lakeshore 7400 vibrating sample magnetometer (VSM), on the substrate temperature of ZnO:Mn thin films exhibiting RTFM. It is evident from Fig. 5 that substrate temperature plays a vital role in good quality ferromagnetic ZnO:Mn thin films. The variation in saturation magnetization (Ms), remnant magnetization (Mr), and coercivity (Hc) along with magnetic moment (μ_B) for different annealing temperatures is presented in Table 1.

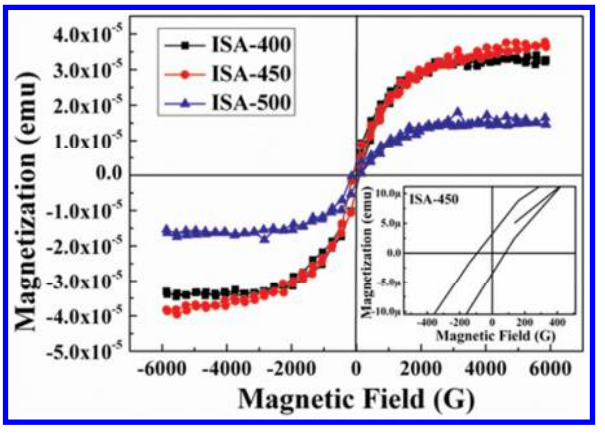

Fig. 5. Field-dependent M-H curves of ZnO:Mn thin films exhibiting RTFM (inset shows clear retentivity).

Temperature-dependent variation in Ms and μ_B/Mn was observed for all the samples. Minimum magnetic moment was observed for thin film grown at substrate temperature of 500 °C (ISA-500). It has been reported that each Mn atom individually has a magnetic moment of about 4.4 μ_B[25] with opposite spin orientation, and the main contribution comes from Mn-3d orbital. The hybridization between O-2p and Mn-3d reduces the magnetic moments compared to that a free Mn atom.[25] In ZnO:Mn, Mn atoms at tetrahedral sites are bonded to four oxygen atoms, thereby reducing the magnetic moment of Mn. The large coordination of oxygen with the presence of O_i enhances the hybridization among the orbitals and the magnetic moment is further reduced accordingly. This can be the possible reason for minimum magnetic moment observed for ISA-500 in which the presence of O_i is supported by RT PL spectra (refer section 3.4). Moreover, the presence of oxygen vacancies, which reduce the crystallinity and the homogenous distribution of localized spins (Mn ions) in the ZnO host matrix are possible reasons for weakening exchange coupling, leading to reduced ferromagnetic signal.

Zinc vacancies are also considered as the possible defects which favor the ferromagnetic exchange interaction. The presence of zinc vacancies in ISA-400 (refer Fig. 4) can be considered as the possible reason for comparatively stronger ferromagnetic response than ISA-500 where no signatures of zinc vacancies are observed. It is reported that in presence of zinc vacancies the Mn d band moves down in energy, causing stronger hybridization between Mn d and ligand p orbitals [26] resulting in stronger nearest-neighbor ferromagnetic exchange interaction in ISA-400 than that of thin film grown at substrate temperature of 500 °C (ISA-500).

Table 1. Variation in magnetic parameters of ZnO:Mn thin films with temperature.

Sample Name	M_s (μemu)	M_r (μemu)	Hc (G)	μ_B/Mn atom ($\times 10^{-3}$)
ISA-400	32.83	3.37	103.82	1.51
ISA-450	37.63	2.96	96.56	1.73
ISA-500	13.68	1.55	128.39	0.63

The maximum value of Ms and μ_B/Mn was achieved for ISA-450, showing stronger ferromagnetic exchange coupling in this sample. The enhanced μ_B/Mn, for ISA-450, is attributed to stoichiometric ZnO (Zn-O bonding), which is favorable for Mn-O-Mn double exchange coupling.[17] At the same time the oxygen diffused into the ZnO host matrix at 450 °C increased the concentration of stoichiometric ZnO for ISA-450 which in turn favors the stability of ferromagnetic ordering [2] (p-d exchange coupling) of Mn in ZnO host matrix leading to enhanced μ_B/Mn atom. Defect mediated RTFM has also been reported by oxygen vacancies[5] in which bound electrons in oxygen vacancies (V_o) couple with Mn ions and cause the ferromagnetic regions to overlap, giving rise to long range ferromagnetic ordering.[27] Since there is no signature of V_o in corresponding DLE spectra (refer Fig. 4) of ISA-450, defect mediated RTFM[28] is ruled out in this sample. Therefore, the improved stoichiometry in ISA-450, with enhanced Zn-O bonding, is possibility considered to be the main source for strong p-d exchange coupling of Mn in ZnO host matrix resulting in enhanced RTFM.

4. Conclusion

In this work, nanocrystalline ZnO:Mn thin films with preferential growth along c-axis were grown on Si substrate under different substrate temperatures using pulsed laser deposition. The structural and compositional analyses reveal that there was an optimum substrate temperature of 450 °C at which the thin film showed stronger texture and better material stoichiometry. The sample grown at substrate temperature of 450 °C (ISA-450) shows (i) improved crystalline quality due to reduced defect density, (ii) enhanced optical quality with minimum contribution from deep level energy transitions, and (iii) enhanced stoichiometric Zn-O bonding with reduced concentration of oxygen vacancies. Moreover, the field-dependent M-H curves revealed enhanced ferromagnetic ordering of 20 nm-sized nanoparticles in ISA-450 with maximum μ_B/Mn. Therefore, it is concluded that ferromagnetic ordering in ZnO:Mn thin films with improved stoichiometry can be enhanced by tailoring the substrate temperature.

Acknowledgments

This project was supported by the AcRF grant (RI 7/08 RSR) provided by NIE, Nanyang Technological University Singapore. One of the authors, Dr Usman Ilyas, is grateful to NIE/NTU for providing research fellowship for this project.

References

1. S. A. Wolf, D. D. Awschalom, R. A. Buhrman, J. M. Daughton, S. von Molnar, M. L. Roukes, A. Y. Ctchelkanova and D. M. Treger, *Science* **294**, 1488 (2001).
2. T. Dietl, H. Ohno, F. Matsukura, J. Cibert and D. Ferrand, *Science* **287**, 1019 (2000).
3. P. Sharma, A. Gupta, K. V. Rao, F. J. Owens, R. Sharma, R. Ahuja, J. M. Osorio, Guillen, B. Johansson and G. A. Gehring, *Nature Materials* **2**, 673 (2003).
4. J. M. D. Coey, M. Venkateshan and C. B. Fitzgerald, Nat. Mater. **4**, 173 (2005).
5. M. El-Hilo and A. A. Dakhel, *J. Magn. Magn. Mater.* **323**, 2202 (2011).
6. E. Przeździecka, E. Kamińska, E. Dynowska, W. Dobrowolski, R. Jakieła, Ł. Kłopotowski, M. Sawicki, M. Kiecana and J. Kossut, *Phys. Stat. Sol. (c)* **3**, 988–991 (2006).
7. C. W. Zou, H. J. Wanga, M. L. Yi, M. Li, C. S. Liu, L. P. Guo, D. J. Fu and T. W. Kang, *Applied Surface Science* **256**, 2453 (2010).
8. H. B. Ruan, L. Fang, G. P. Qin and C. Y.Kong, in *3rd IEEE International NanoElectronics Conference*, edited by P. Chu (IEEE, City Univ Hong Kong, Hong Kong, PEOPLES R CHINA, 2010), Vol. 1-2, pp. 1088-1089.
9. F. Pan, C. Cong, X. J. Liu, Y. C. Yang and F. Zeng, *Mater. Sci. Eng.* **R 62**, 1 (2008).
10. K. Potzger and S. Q. Zhou, *Phys. Stat. Sol. B* **246**, 1147 (2009).
11. R. P. Davies, C. R. Abernathy, S.J. Pearton, D. P. Norton, M. P. Ivill and F. Ren, *Chem. Eng. Comm.* **196**, 1030 (2009).
12. U. Ilyas, R. S. Rawat, G. Roshan, T. L. Tan, P. Lee, S. V. Springham, S. Zhang, L. Fengji, R. Chen and H. D. Sun, *Appl. Surf. Sci.* **258**, 890 (2011).
13. U. Ilyas, R. S. Rawat, T. L. Tan, P. Lee, R. Chen, H. D. Sun, L. Fengji and S. Zhang, *J. Appl. Phys.* **110**, 093522 (2011).
14. X. J. Liu, C. Song, F. Zhang, X. B. Wang and F. Pan, *J. Phys. D: Applied Physics* **40**, 1608 (2007).
15. X. Yong Li, H. Jian Li, M. Yuan, Z. Jun Wang, Z. You Zhou and R. B. Xu, *Journal of Alloys and Compounds* **509**, 3025 (2011).
16. P.T. Hsieh, Y.C. Chen, K.S. Kao and C.M. Wang, *Applied Physics A Material Science and Processing* **90**, 317 (2008).
17. U. Ilyas, R. S. Rawat, T. L. Tan, P. Lee, R. Chen, H. D. Sun, L. Fengji and S. Zhang, *J. Appl. Phys.* **111**, 33503 (2012).
18. Y. Y. Chen, J. C. Hsu, C. Y. Lee and P. W. Wang, *Journal of Material Science* **48**, 1225 (2013).
19. Y. Y. Tay, S. Lib, C. Q. Sun and P. Chen, *Appl. Phys. Lett.* **88**, 173118 (2006).
20. M. Khalid, M. Ziese, A. Setzer, P. Esquinazi, Lorenz, H. Hochmuth, M. Grundmann, D. Spemann, T. Butz, Brauer, W. Anwand, G. Fischer, W. A. Adeagbo, W. Hergert and A. Ernst, *Phys. Rev. B* **80**, 035331 (2009).
21. N. Gopalakrishnan, L. Balakrishnan, B. Srimathy, M. Senthil Kumar and T. Balasubramanian, *Phys. Status Solidi A* **207**, 2180 (2010).

22. M. S. Oh, S. H. Kim and T. Y.Seong, *Appl. Phys. Lett.* **87**, 122103 (2005).
23. L. Schmidt-Mende and L. Macmanus-Driscoll, *J. Materials Today* **10**, 40 (2007).
24. U. Ilyas, R. S. Rawat, Y. Wang, T. L. Tan, P. Lee, R. Chen, H. D. Sun, F. Li and S. Zhang, *Appl. Surf. Sci.* **258**, 6373 (2012).
25. Q. Wang, Q. Sun, B. K. Rao and P. Jena, *Phys. Rev. B* **69**, 233310 (2004).
26. D. Iusan, B. Sanyal and O. Eriksson, *Phys. Rev. B* **74**, 235208 (2006).
27. S. J. Pearton, D. P. Norton, M. P. Ivill, A. F. Hebard, J. M. Zavada, W. M. Chen and I. A. Buyanova, *Journal of Electronic Materials* **36**, 462 (2007).
28. U. Ilyas, T. L. Tan, P. Lee, R. V. Ramanujan, Fengji Li, Sam Zhang, R. Chen, H. D. Sun and R. S. Rawat, *Journal of Magnetism and Magnetic Materials* **344**, 171 (2013).